JOURNAL OF GEOPHYSICAL RESEARCH, VOL. 101, NO. D4, PAGES 9001-9015, APRIL 20, 1996

Space-time variations in water vapor as observed by the UARS Microwave Limb Sounder

Lee S. Elson, William G. Read, and Joe W. Waters

Jet Propulsion Laboratory, California Institute of Technology, Pasadena

Philip W. Mote, Jonathan S. Kinnersley,[1] and Robert S. Harwood

The University of Edinburgh, Edinburgh, Scotland

Abstract. Water vapor in the upper troposphere has a significant impact on the climate system. Difficulties in making accurate global measurements have led to uncertainty in understanding water vapor's coupling to the hydrologic cycle in the lower troposphere and its role in radiative energy balance. The Microwave Limb Sounder (MLS) on the Upper Atmosphere Research Satellite is able to retrieve water vapor concentration in the upper troposphere with good sensitivity and nearly global coverage. An analysis of these preliminary retrievals based on 3 years of observations shows the water vapor distribution to be similar to that measured by other techniques and to model results. The primary MLS water vapor measurements were made in the stratosphere, where this species acts as a conserved tracer under certain conditions. As is the case for the upper troposphere, most of the stratospheric discussion focuses on the time evolution of the zonal mean and zonally varying water vapor. Stratospheric results span a 19-month period and tropospheric results a 36-month period, both beginning in October of 1991. Comparisons with stratospheric model calculations show general agreement, with some differences in the amplitude and phase of long-term variations. At certain times and places, the evolution of water vapor distributions in the lower stratosphere suggests the presence of meridional transport.

1. Introduction

Water vapor (H_2O) plays several important roles in the atmosphere. In the troposphere, phase changes and radiative properties cause it to dominate processes crucial to energy balance. Therefore determination and prediction of climate change will depend heavily on accurate measurements of water vapor, especially in the upper troposphere. The significance of upper tropospheric H_2O stems from *Lindzen's* [1990] controversial suggestion that a future increase in surface temperatures would probably result in a decrease in upper tropospheric H_2O. *Gutzler* [1993] reported that current uncertainty in upper tropospheric humidity (UTH) results in an uncertainty in the upwardly directed infrared radiance at the tropopause, that is of the same magnitude as the radiative change due to a doubling of carbon dioxide. Clearly, the extent to which upper tropospheric water vapor is coupled to boundary layer convection is important in studies of climate and climate change.

The upper troposphere acts as a crucial link between the surface, where many wave variations have their origins, and the stratosphere where changes are driven mostly by wave activity. Good examples of this are the semiannual and quasi-biennial oscillations (SAO and QBO, respectively) which are influenced by upward propagating planetary waves. The detection and quantification of such waves help to complete our understanding of how changes are forced in the stratosphere. The upper troposphere also exhibits shorter-period oscillations, such as the 30-to 60-day or Madden and Julian oscillation [*Madden and Julian*, 1994], which are driven by and indicative of interactions between convection and the circulation.

Water vapor, like related quantities such as rainfall, varies on a variety of spatial and temporal scales. This can make observations difficult to interpret. In the upper troposphere, in situ measurements provide high vertical resolution, but their usefulness is limited, due in part to measurement inaccuracies of relative humidity sensors on conventional radiosondes [*Wade*, 1994]. From other measurements, such as lidar and Loran tracked soundings [*Soden et al.*, 1994], we know that

[1]Now at Department of Applied Mathematics, University of Washington, Seattle.

Paper number 95JD03653.
0148-0227/96/95JD-03653$05.00

UTH can have vertical structure of the order of 1 km, especially in the vicinity of ice clouds, which act as a vapor source [*Smith et al.*, 1994]. Although such structure is beyond the ability of current satellites to measure, satellites have the advantage of much greater horizontal and temporal coverage and resolution, and the number of satellites observing UTH is growing. Satellite observations can be separated into two categories: nadir and limb measurements. Limb sounders view the atmosphere tangentially at its limb, while nadir sounders view in a direction closer to perpendicular to the surface. Nadir-viewing instruments can be further subdivided according to whether they are in low or high orbit. High orbit, geostationary sensors such as the GOES 6.7-μm channel make possible the determination of UTH [*Soden and Bretherton*, 1993; *Udelhofen and Hartmann*, 1995] and offer excellent (about 10 km) horizontal resolution but limited horizontal coverage. GOES is sensitive to UTH between 500 and 200 hPa (5.5-12 km) and therefore may not be able to distinguish between vertical variations on smaller scales and horizontal or temporal variations. Similar restrictions apply to H_2O retrieved from the High Resolution Infrared Radiation Sounder 2 (HIRS2) on the low-altitude, polar-orbiting TIROS satellites [*Susskind*, 1993]. HIRS2 observations, because of the orbit, cover the entire globe daily, but the effective horizontal resolution is less than that of GOES. Although the field of view (FOV) is of the order of 10-50 km, retrievals have a spacing of about 250 km [*Susskind et al.*, 1984].

Limb sounders provide better vertical resolution than nadir sounders. The Microwave Limb Sounder (MLS) [*Barath et al.*, 1993] on the Upper Atmosphere Research Satellite (UARS) was designed to sense water vapor in the stratosphere using measurements at 183 GHz [*Lahoz et al.*, 1996b]. Its 205-GHz radiometer is most sensitive to H_2O in the upper troposphere where the concentration is in the range 100-300 parts per million by volume (ppmv) [*Read et al.*, 1995]. Preliminary values of water vapor on a 215-hPa surface have been retrieved using this radiometer and are presented here. The 215-hPa surface was chosen in order to emphasize the high values of H_2O in the tropics. In the polar regions, where the tropopause is low, most of these measurements are in the stratosphere. While the failure of the 183-GHz radiometer in April 1993 limits the stratospheric H_2O data set to about 19 months, the 205-GHz radiometer has made 3 years of nearly continuous measurements and continues to function. With a 3-km FOV in the vertical and retrievals that have little degradation due to cirrus clouds, MLS provides a water vapor data set with some advantages over those previously mentioned. There are also some disadvantages. Like most limb sounders, horizontal resolution in the cross-track direction is limited by the orbital spacing and therefore by the orbital period. For MLS, there are about 15 orbits per day, with adjacent orbits separated by about 2670 km at the equator. Although the preliminary H_2O retrievals discussed here have not yet been systematically validated, Read et al. show that the comparison between daily MLS H_2O observations and related model and satellite results is quite good. Read et al. also compared horizontally binned data for 3-month periods with cloud climatologies and found that the two had similar morphologies. *Elson et al.* [1994b] compared "synoptic" (see below) maps of MLS water vapor with the GOES data described above and found the morphological agreement to be reasonable, given the significant differences in horizontal and temporal resolution in the two data sets. *Newell et al.* [1996a] compared upper tropospheric aircraft observations of H_2O with those of MLS and found generally good agreement, with a tendency for MLS values to be too high for mixing ratios less than 200 ppmv. Comparisons between areas of rising (sinking) motion inferred from European Centre for Medium-Range Weather Forecasts (ECMWF) analyses and moist (dry) MLS observations in the tropical Pacific by *Newell et al.* [1996b] showed the two to be similar.

In the stratosphere, the circulation is frequently described in terms of its residual mean, which at low altitudes, consists of upwelling at low latitudes and a downward return flow at high latitudes. Superimposed on this flow are various cycles: the QBO, SAO and annual cycle. There have been numerous attempts to use long-lived species as tracers of motions associated with these cycles. Two factors can complicate this process. Different tracers often yield conflicting results, and the cycles can influence one another. A good example of this is the QBO. The circulation associated with this phenomenon is confined to the equator and subtropics and is strongest between about 10 and 40 hPa [*Andrews et al.*, 1987]. Several workers [e.g., *Chipperfield and Gray*, 1992] have noted that the sign of the QBO anomaly for a particular tracer depends on the direction and sign of the mixing ratio gradient of that tracer. A recent publication [*Hasebe*, 1994] finds that ozone and aerosols do not give a consistent picture of the QBO when compared with model predictions.

H_2O in the stratosphere has also been used as a tracer of air motion, since at lower levels, it is usually conserved on timescales less than about a hundred days [*Le Texier et al.*, 1988]. Limb Infrared Monitor of the Stratosphere (LIMS) observations show that the general characteristics of the vertical distribution of H_2O in the upper stratosphere are consistent with methane acting as a source [*Jones et al.*, 1986]. *Lahoz et al.* [1996b] have shown that the 183-GHz radiometer on MLS provided H_2O measurements in the stratosphere that have, for the version 3 data used here, a single profile precision of 5% or better and an accuracy of 1.2 ppmv or better between 46 hPa and .46 hPa. By comparing version 3 retrievals with correlative data, they were able to estimate that MLS H_2O observations may be too high by about 5-20%, depending on pressure level. This must be kept in mind when comparing MLS observations to LIMS, as is done here. Transport in the winter polar vortices was examined by *Lahoz et al.* [1994, 1996a] using individual vertical profiles of MLS H_2O along an orbit track for selected days. *Harwood et al.* [1993] studied transport of H_2O out of the southern winter vortex to midlatitudes. Focusing on the equatorial regions and subtropics, *Carr et al.* [1995] noted that MLS observa-

tions confirm a H_2O distribution generally consistent with the Brewer-Dobson circulation modulated by the annual cycle, the SAO and the QBO. They examined the lower stratosphere (pressures greater than 20 hPa) and found a significant annual variation. *Mote et al.* [1995] demonstrated that this variation was largely due to the annual variation in tropical tropopause temperature that controls the mixing ratio of air entering the stratosphere.

The discussion that follows is concerned with the spatial variations of MLS H_2O in the upper troposphere and stratosphere and how these variations change with time. We examine both the zonal mean and the deviations from the mean. Measurements in the upper troposphere are relatively new and unique. Their general characteristics will be compared with similar observations and with models. MLS stratospheric observations will also be compared with model calculations, with emphasis on vertical displacement of H_2O isosurfaces. Although the results presented here are meant to serve as an overview, several periods will be examined in greater detail.

Section 2 briefly describes the analysis used with the MLS data and section 3 contains results from 3 years of upper tropospheric measurements of H_2O, including model comparisons. Section 4 examines the stratosphere at several levels in the vertical and compares equatorial behavior with that of a two dimensional (2-D) model and section 5 contains a discussion of other observations and some conclusions.

2. Data Analysis

The orbit of UARS causes measurements made by MLS to progress through all local solar times in about 36 days. In order for side-looking instruments to cover the high latitudes of both hemispheres, UARS performs a 180° yaw maneuver after covering all local times. The period between yaws is referred to as a UARS "month." MLS views all longitudes daily, although the latitudinal sampling depends on the UARS yaw state.

One way to quantify the large-scale variability of a satellite data set is to use Fourier analysis. This approach has been applied here in the time and longitude domain, while spatial binning is applied to the height and latitude domains. *Elson and Froidevaux* [1993] described the technique and *Elson et al.* [1994a] applied it to ozone (O_3) variations. Specifically, this approach starts with a coordinate system rotation that allows the determination of Fourier transform coefficients of H_2O concentration for discrete values of m, the longitudinal wavenumber, and σ, the frequency at specific latitudes and heights. The use of fast Fourier transforms (FFTs) requires that data points be equally spaced in longitude and time. Because of this and variations in the UARS orbital period, analysis of data over extended periods of time is generally not possible. These variations are small enough to allow the calculation of Fourier coefficients over a 7.2-day (108 orbit) period and unless otherwise indicated, these coefficients are used here. Longer calculations (e.g., over a UARS month) are possible only during times when the orbital period is very slowly changing. The Fourier transform coefficients can be used to create "synoptic" maps, i.e., a gridded array calculated by inverting the coefficients for all longitudes at one time. The 15 UARS orbits per day result in a Nyquist period near 1 day at the equator for the smaller longitudinal wavenumbers (largest spatial scales), while the largest resolvable wavenumber (6, corresponding to about 6600 km at the equator) has a slightly longer Nyquist period. Therefore the diurnal frequency, which could be important in the upper troposphere but not (for H_2O) in the stratosphere, will not be fully resolved, resulting in the possibility of aliasing. Small scale spatial variability may cause a similar result. Despite these limitations, daily maps of water vapor in the upper troposphere (and stratosphere) appear reasonable [*Elson et al.*, 1994b]. The likely reason for this is that there does not appear to be much power at the diurnal frequency. *Udelhofen and Hartmann* [1995] found that diurnal amplitudes in UTH are typically only a few percent.

The results presented here consist largely of time variations in the zonally averaged and zonally varying (wavenumbers 1-6) H_2O concentration. These variations are calculated by combining all resolved frequency contributions to the inverse transform for individual zonal harmonics. As discussed by *Elson et al.* [1994a], the Fourier transform coefficients are also used to calculate the cross-spectral and power spectral density functions, as well as estimates of statistical significance in the form of a posteriori probability and eastward and westward propagating wave variances described by *Schäfer* [1979].

3. Upper Tropospheric Results

3.1 Time Evolution of Zonally Averaged H_2O

The zonally averaged ($m = 0$) evolution of MLS H_2O at 215 hPa for the first 3 years of measurements is shown in Plate 1. Missing days (e.g., UARS yaw maneuvers, MLS field-of-view interference from the Moon, and platform and instrument problems) have been omitted, resulting in gaps in this and similar plates. A great deal of day-to-day variability, as well as a clear annual cycle, are evident. The maximum in concentration occurs, as expected, in the equatorial regions and its latitude tends to follow the Sun with a lag of about 2 months. The poleward deflection of the maximum is similar in the two hemispheres and reaches its extreme in February and August in the south and north, respectively. Maximum values are usually greatest in June, July and August, as expected from the greater convective activity that occurs over land and the larger land mass in the northern hemisphere. A weak splitting of the maximum tends to appear in November, especially in 1991. This is likely due to differences between eastern and western hemispheres, as described below. The largest meridional gradients occur in the subtropics and there is considerable interannual variation, with 1992-1993 be-

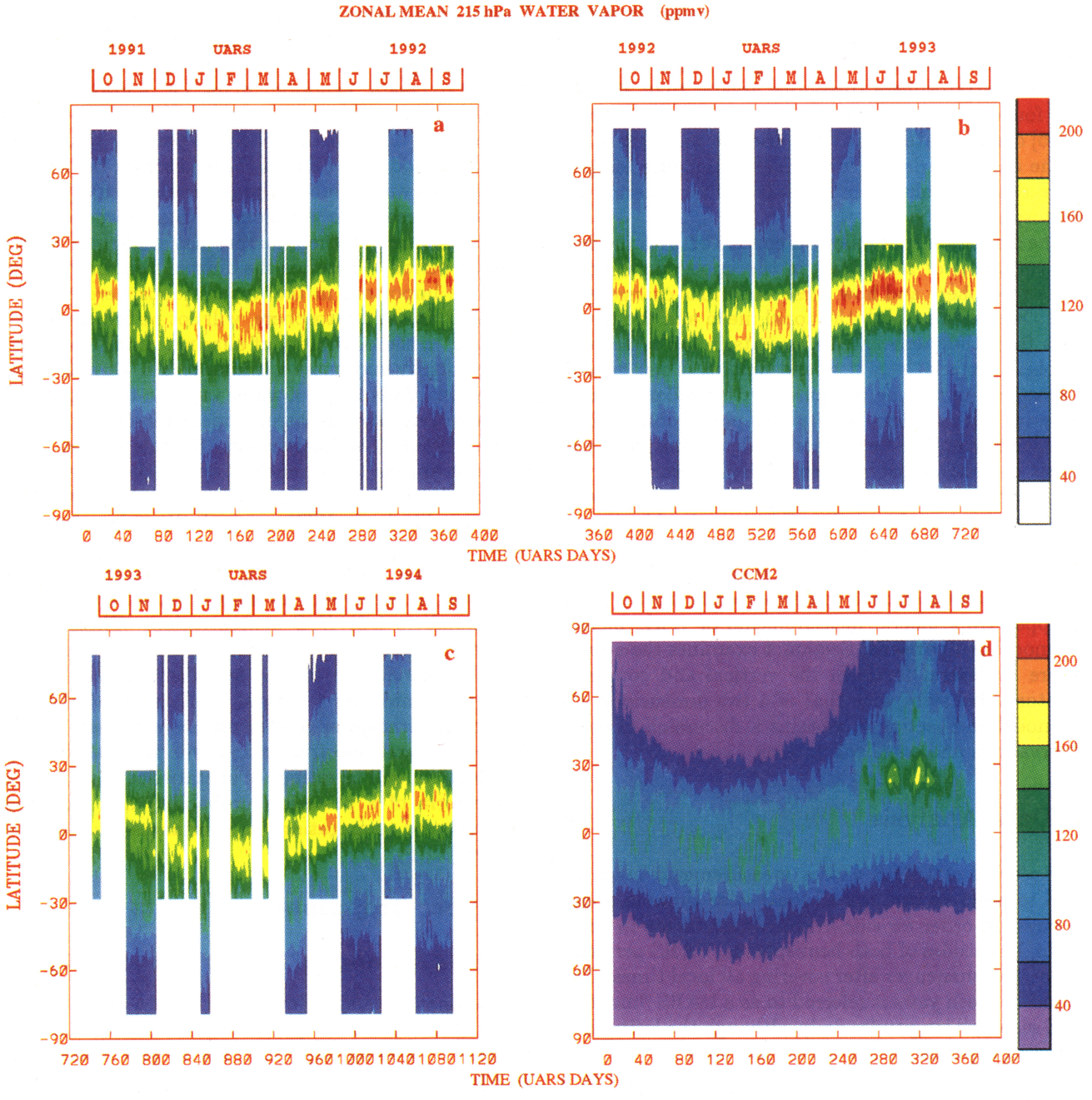

Plate 1. Time evolution of zonal mean 215 hPa MLS water vapor (in parts per million by volume) for (a) UARS days 20-375 (October 1, 1991 to September 20, 1992), (b) UARS days 380-736 (September 25, 1992 to September 16, 1993), (c) UARS days 743-1095 (September 23, 1993 to September 10, 1994), and (d) CCM2 model results. MLS values less than 40 in parts per million by volume are shown in white to indicate that they are more uncertain than higher values.

ing slightly wetter than 1991-1992 and 1993-1994 being significantly drier than either of the 2 previous years. By "interannual variation," we mean changes occurring on timescales longer than a year that are not obviously associated with known phenomena.

Plate 1 also shows calculations of zonally averaged H_2O, described by *Mote* [1995], from the National Center for Atmospheric Research Community Climate Model (CCM2). The overall structure of the model variations is similar to the observations; however, the model tends to predict a larger increase in the maximum concentration in July and August than is observed. This feature was noted by *Soden and Bretherton* [1994] in their comparison of CCM2 simulations and GOES data. Soden and Bretherton also suggested that the CCM2 underestimates the gradient in H_2O between

the equator and subtropics owing to difficulties in simulating ascent and descent in the Hadley circulation. Larger gradients and maxima closer to the equator in MLS data in July and August support this conclusion. The model also produces a maximum in the concentration that is farther north than that observed during the northern summer months. *Salathé and Chesters* [1995] and *Salathé et al.* [1995] found similar differences when comparing TIROS Operational Vertical Sounder data with both ECMWF analyses and Goddard Laboratory for Atmospheres General Circulation Model simulations. In both cases, they found that, as here, observations tend to show more moisture where values are large. They suggest that this is due in part to the convective parameterization schemes used by the model.

3.2 Time Evolution of Zonally Varying H_2O

Significant departures from the zonal symmetry in the H_2O field just described are also present. In searching for waves, two competing factors influence the way data are analyzed. If one is searching for short-period (less than 10 days) waves, it is useful to examine multiple short periods (about 30 days). The reason for this is that transience in longer records may obscure signals [*Salby et al.*, 1984]. The limited spectral resolution is not usually a serious constraint. If longer-period variations, such as the 30-to 60-day oscillation, are to be analyzed, good spectral resolution is important and available only through the use of much longer records [*Salby and Hendon*, 1994]. Because the initial stages of analysis of MLS data limit records to about 30 days, only a few attributes of long- period oscillations are evident in the results below. Most of the discussion will focus on shorter-period waves.

Plate 2 shows 215-hPa wave variance obtained from zonal Fourier coefficients for one UARS month (January 10 to February 8, 1993). This time was chosen because the slow variation of the UARS orbit during this period makes possible an extended FFT calculation. Both eastward and westward propagating wave variances are depicted as a function of latitude and frequency for each resolvable zonal wavenumber (1-6). Because the variance field has been spectrally smoothed [*Elson et al.*, 1994a] and the amplitude variation with small frequency is rapid, values within one spectral bandwidth on either side of zero frequency are distorted and have been omitted. Plate 2a (wave 1) indicates the presence of the diurnal signal that, as discussed above, may be aliased to some extent and large-amplitude variances within a few degrees of the extremes in latitude coverage are possibly artifacts of the transform process [*Elson and Froidevaux*, 1993]. This plate reveals that for small wavenumbers (large scales), most of the power is present at low frequencies and that most of these long-period disturbances propagate eastward. The latitudinal extent of all disturbances is quite limited. The larger wavenumbers show evidence of faster, primarily eastward moving peaks, with periods as short as about 1.5 days. Calculations of a posteriori probability, made from estimates of coherency, show that peaks marked with red arrows are statistically significant at the 90% or greater level. Although significant, some of the peaks are quite small (amplitudes about 10 ppmv) and may reflect transient behavior rather than regular long-term propagation. One other month (August 13 to September 20, 1992) has been examined and shows similar behavior for low frequencies but fewer high- frequency variations.

4. Stratospheric Results

4.1 Time Evolution of Zonally Averaged H_2O

The zonally averaged ($m = 0$) evolution of H_2O, from October 1991 to April 1993, is shown in Plate 3 for four different levels in the stratosphere. Several features are prominent in the data. In the equatorial region, the SAO becomes more visible as one progresses upward in the atmosphere. At 2 hPa, the SAO dominates the pattern between 30°N and 30°S but is replaced by an irregular annual variation in the polar region. This annual component is due in part to variations in vertical motion there [*Lahoz et al.*, 1994]. As high H_2O values descend, concentrations at and above 2 hPa increase. A strong annual cycle in the tropics, especially clear at 22 hPa, is largely due to annual variations in H_2O mixing ratio at the tropopause [*Mote et al.*, 1995]. At low latitudes, there is also evidence of interannual change at all levels. During the second year, the tropics are drier at 46 hPa and wetter at 10 and 2 hPa. As noted by *Carr et al.* [1995], the tropical mixing ratio at 22 hPa has a variation that is not annual. Enhanced dehydration over the Antarctic is evident at 46 hPa in August and September of 1992. This is expected because of removal of H_2O by Type II polar stratospheric clouds [e.g., *Kelly et al.*, 1989].

Another view of the SAO is provided by time series versus altitude plots at the equator. Plates 4a and 4b show zonally averaged MLS O_3, (discussed below) while Plates 4c and 4d show the corresponding H_2O observations. Plate 4e displays the results from a 2-D model simulation for 1 year starting on UARS day 1 (September 12, 1991). The model is an improved version of that described by *Kinnersley and Harwood* [1993]. It has a prescribed water vapor mixing ratio at the 60-km (about 0.2 hPa) level and at the tropopause. The general form of the observations and model agree. The most obvious differences are in the amplitude of variations, or the displacement of the isopleths in the upper stratosphere, and in the timing of the second maximum (June or July in the observations, April or May in the model). The observed amplitudes are larger than the model above about 4 hPa. At 10 hPa, the model shows variations on a timescale of a few months that do not appear in the first 10 months of observations.

4.2 Time Evolution of Zonally Varying H_2O

Plate 5 shows the absolute value of wavenumber 1 variations, at pressure levels of 46, 10 and 2 hPa. Wave activity is strongest at high latitudes in the fall, winter

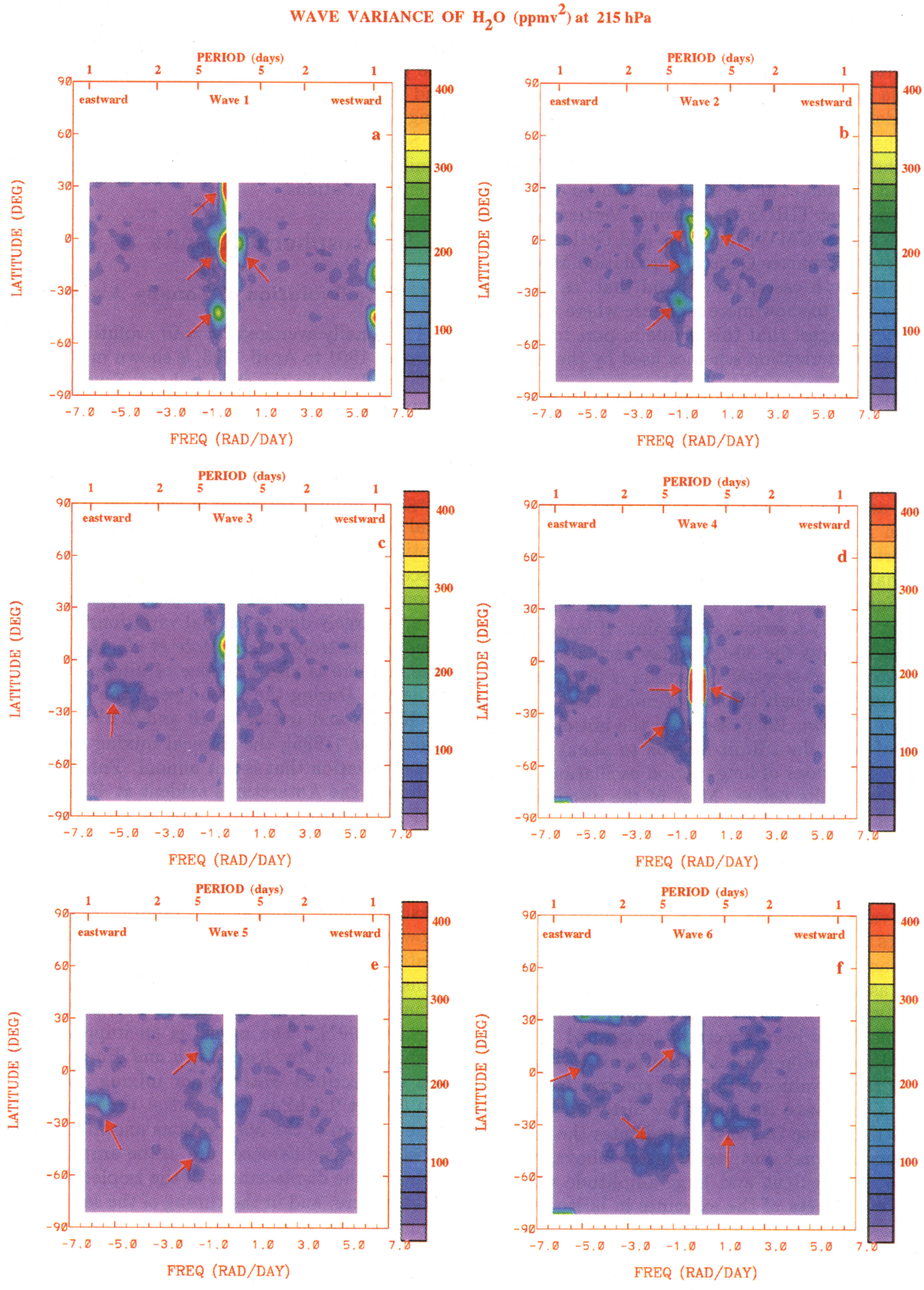

Plate 2. Spectrally smoothed wave variance of water vapor (in parts per million by volume squared) at 215 hPa, as a function of latitude and frequency for zonal wavenumbers 1-6 (Plates 2a-2f, respectively). Arrows mark regions where statistical significance exceeds 90%. Data from January 10 to February 8, 1993 were used in the analysis.

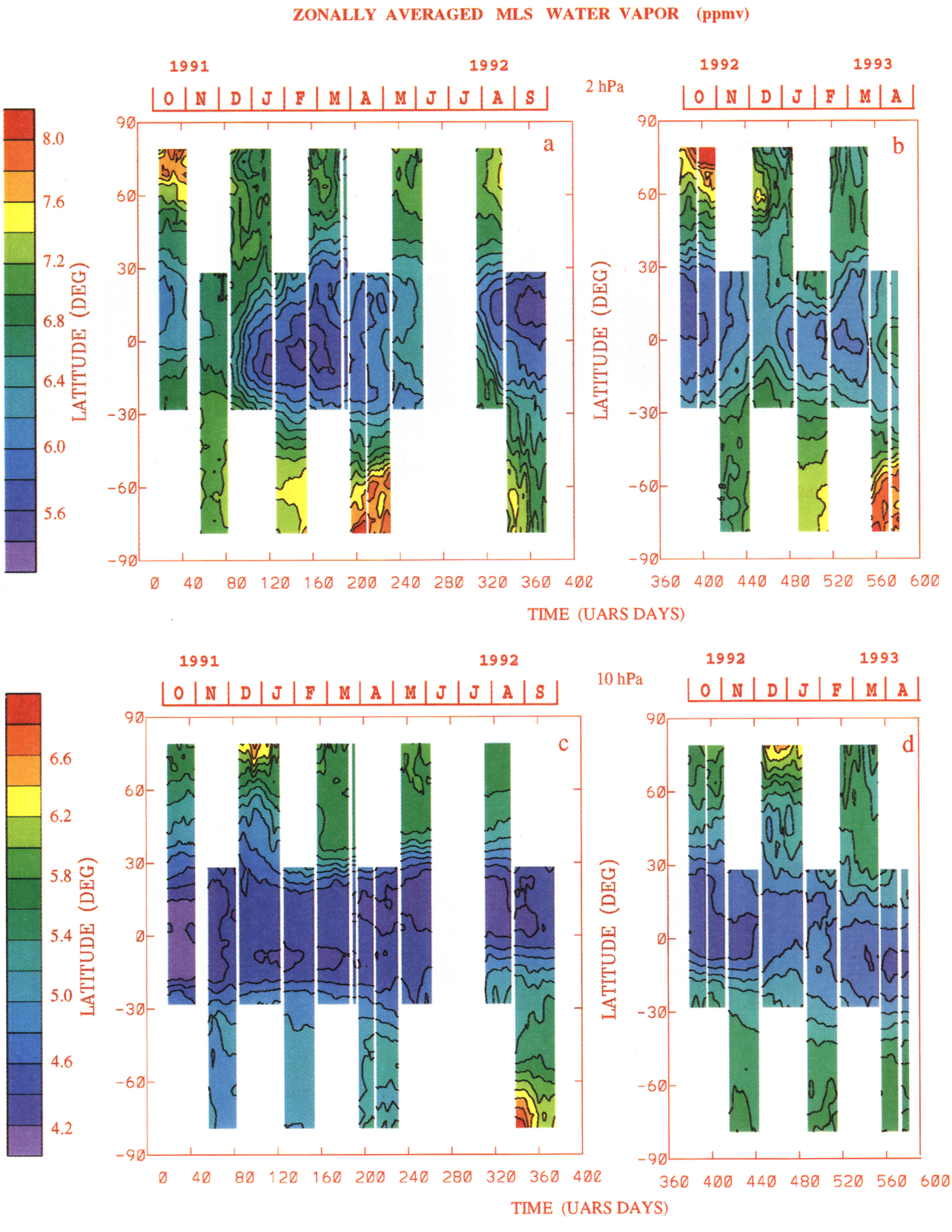

Plate 3. Time evolution of zonal mean MLS water vapor (in parts per million by volume) at (a) 2 hPa for UARS days 20-375 and (b) 2 hPa for UARS days 380-582. Plates 3c and 3d are the same as Plates 3a and 3b but at 10 hPa. Plates 3e and 3f are the same as Plates 3a and 3b but at 22 hPa. Plates 3g and 3h are the same as Plates 3a and 3b but at 46 hPa. A 5-day running mean has been applied to the data.

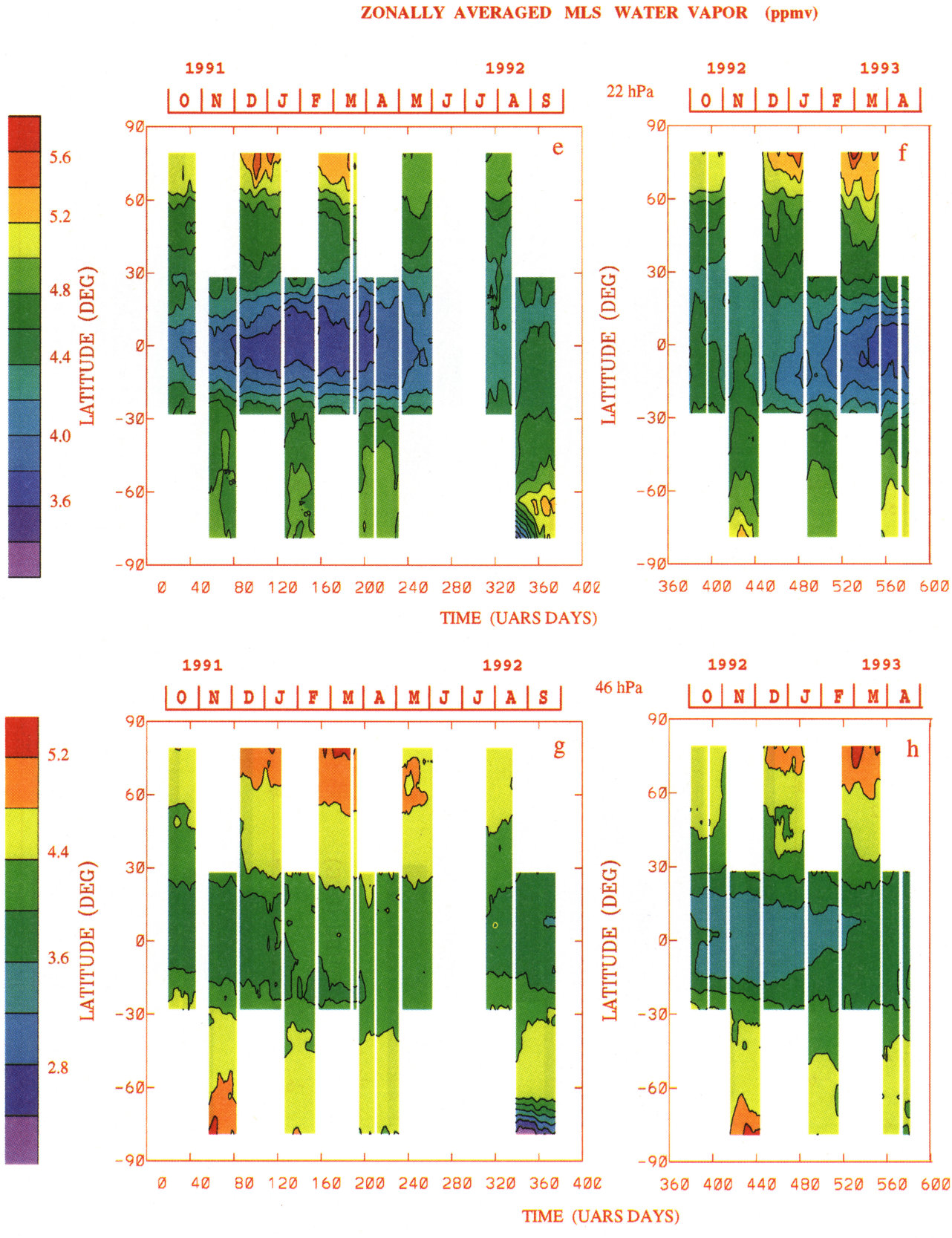

Plate 3. (continued)

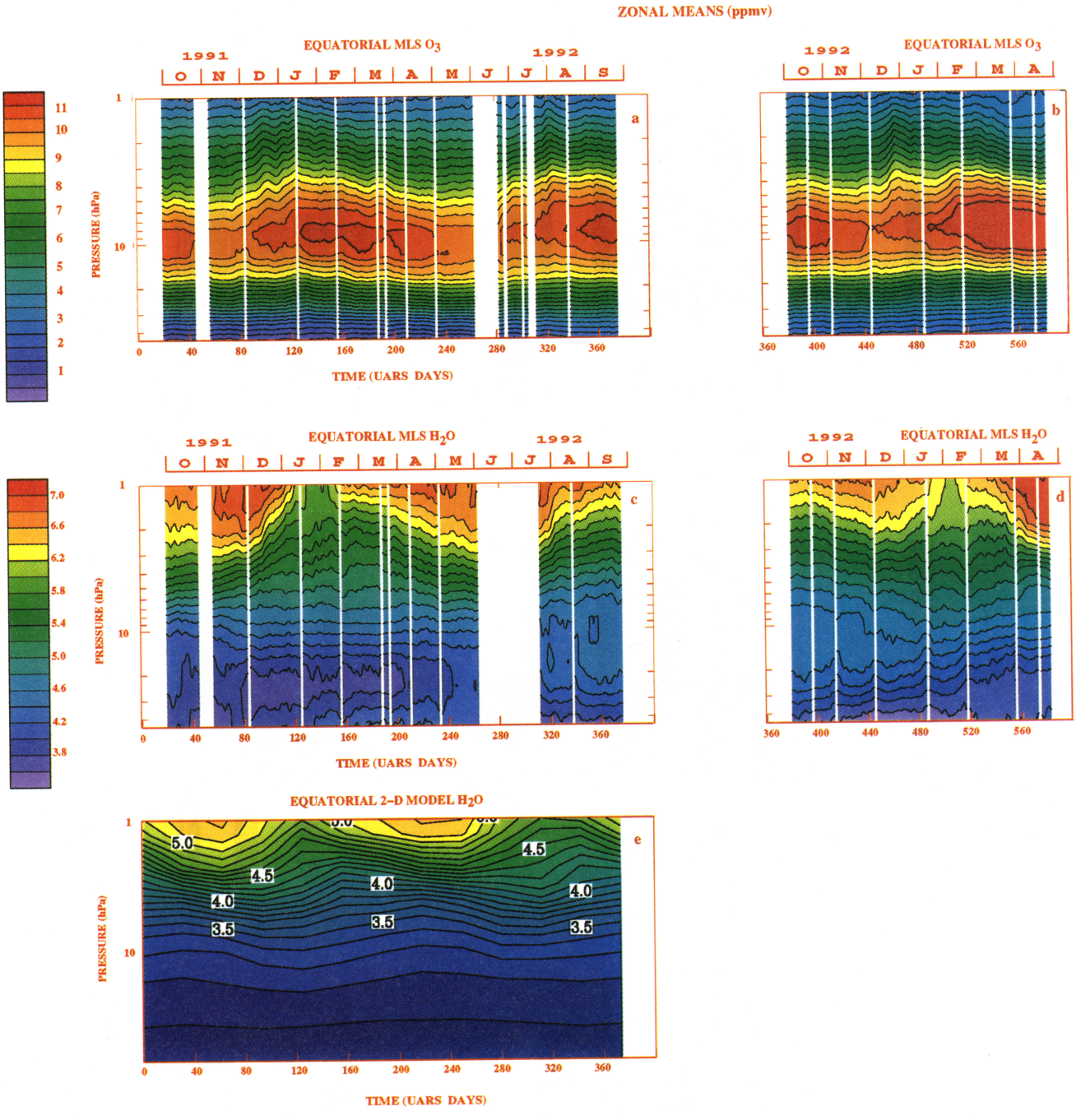

Plate 4. Equatorial zonal mean ozone (in parts per million by volume) versus pressure and time, smoothed with a 3 day running mean, for (a) the first year of MLS measurements, and (b) for the second year. Plates 4c and 4d are the same as Plates 4a and 4b but for water vapor. Plate 4e shows results from 2-D model calculations.

and spring months, but occurs in bursts lasting from one to several weeks. The largest amplitudes occur at high latitudes during winter (August 1992 at 46 hPa in the south and December 1991 to January 1992 at 10 hPa in the north). This is a manifestation of the dehydration of the polar vortex (section 4.1) coupled with small displacements of the center of the vortex from the pole. Smaller but significant wave amplitudes can be seen at all levels during August and September 1992 at southern middle and high latitudes. These features are a result of enhanced wave activity that transports high ozone and low water vapor from low to high latitudes, as discussed by *Elson and Froidevaux* [1993]. Plate 5 may be directly compared with Figure 1 of *Elson et al.* [1994a], which shows $m = 1$ variations in O_3. The overall structure of variations is similar for the two species; however, an examination of specific events shows that the relative amplitude is often larger

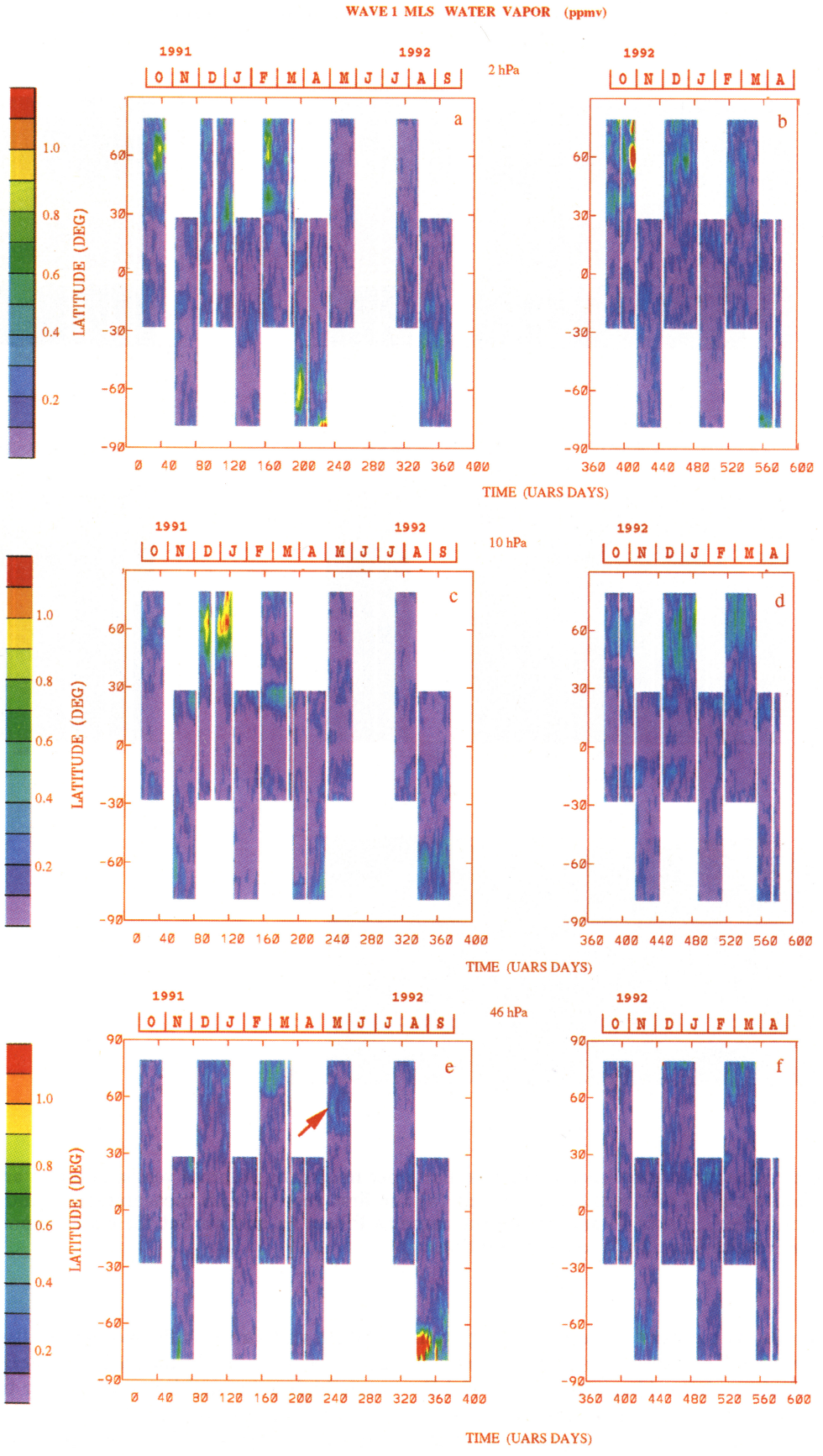

Plate 5. As in Plate 3 but for zonal wavenumber 1 water vapor amplitude (in parts per million by volume). The 22-hPa results have been omitted.

in one species than the other. Which species has the stronger response depends on factors that influence the concentration. At 2 hPa, O_3 is primarily photochemically controlled and H_2O is primarily dynamically controlled, so that a large temperature amplitude in the absence of advection might be expected to produce larger O_3 variations. At lower altitudes, where both species are dynamically controlled, differences are due to the background (zonally averaged) distribution of the two species in the presence of transport. For example, at 46 hPa, the water vapor wave 1 amplitude is large near 60°N in May 1992 (marked with a red arrow in Plate 5e). The O_3 amplitude for the same time and place is small. An examination of a vertical cross section of the zonal mean of the two species, in Figure 1, shows why this occurs. The distribution of O_3 is not unusual, with relatively small meridional gradients in this region. The H_2O distribution, however, shows a small anomalous peak near 60° with isopleths nearly perpendicular to those of O_3. The associated increase in meridional gradient equatorward of this feature means that a zonally asymmetric meridional wind is more likely to produce meridional transport and a zonal asymmetry in the distribution. An examination of National Meteorological Center data shows an enhancement in the meridional wind at this time and place.

At higher altitudes, water vapor is conserved over a period of several weeks and can therefore act as a tracer of atmospheric motions for these timescales. For example, in Plate 5 at 2 hPa, the wave 1 amplitudes for days 338-375 show considerable activity between 30° and 60°S. During this UARS month, the orbital period was stable enough to allow the calculation of one set of Fourier coefficients for the entire month. Figure 2 shows both the zonal mean and the wave 1 variance for a part of the spectrum centered on an eastward 10-day period. The region near 2 hPa, which shows a peak in the variance, corresponds to the region that has the largest component of zonal mean gradient in the meridional direction. Therefore it is likely that meridional transport is effective at this time and place. The results for $m = 2$ fluctuations (not shown) are similar in structure to those for $m = 1$, but the amplitudes are generally smaller. In the future, other large-amplitude features in Plate 5 will be analyzed using more sophisticated techniques.

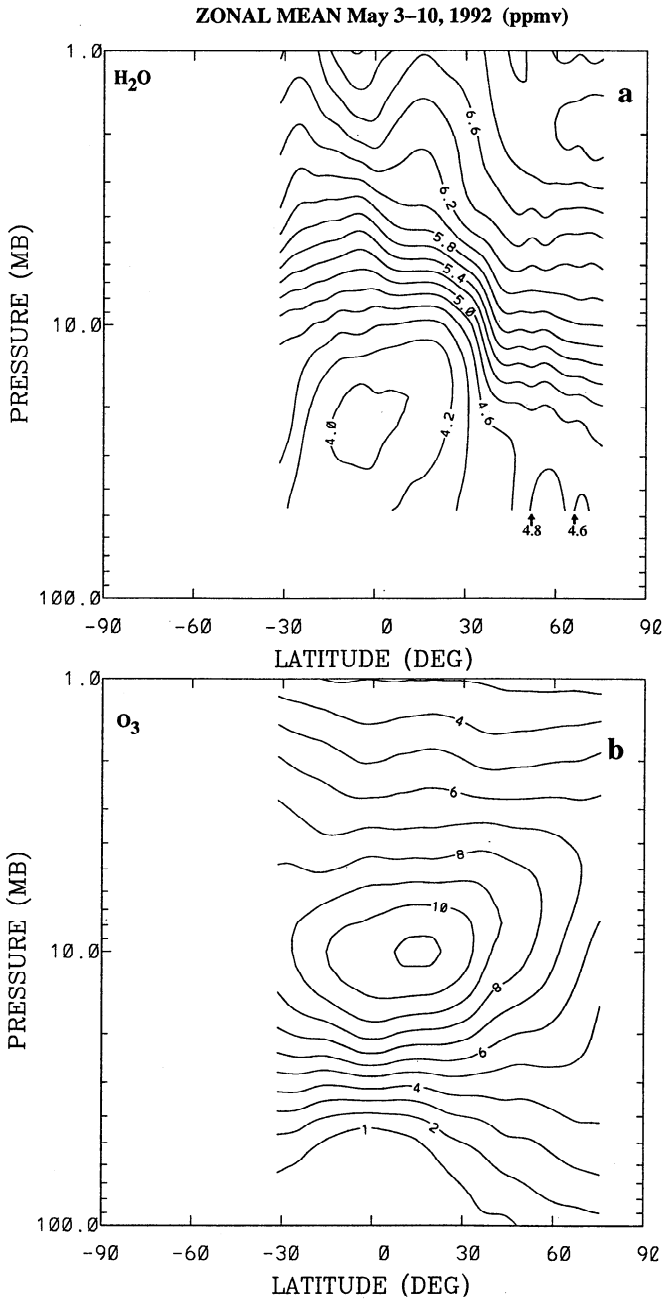

Figure 1. Zonal mean values of (a) water vapor and (b) ozone (in parts per million by volume) versus pressure and latitude for May 3-10, 1992.

5. Discussion

5.1 The Upper Troposphere

The tropospheric variations in zonal mean H_2O shown above are similar to the HIRS2 results of *Susskind* [1993, Figure 7b], despite the differences in measurement technique and geometry. The implication from the 3 years of MLS data and 1 year of HIRS2 data is that the seasonal variations and hemispheric asymmetries depicted are fairly robust features. Susskind also used HIRS2 data to show that hemispheric asymmetries in the seasonal variation of zonal mean H_2O are dependent on the longitude range over which the average was calculated. For example, he found that most of the differences in peak values between January and July are due to differences in the longitude range from 150°W eastward to 30°E. *Soden and Bretherton* [1994] noted substantial differences between midlatitude GOES UTH data over this region and SAGE II (Stratospheric Aerosol and Gas Experiment) observations that covered all longitudes. Satellite observations of the location of the intertropical convergence zone [*Waliser and Gautier*, 1993] also show hemispheric asymmetries. A global average of 17 years of highly reflective cloud data bears a striking resemblance to Plate 1.

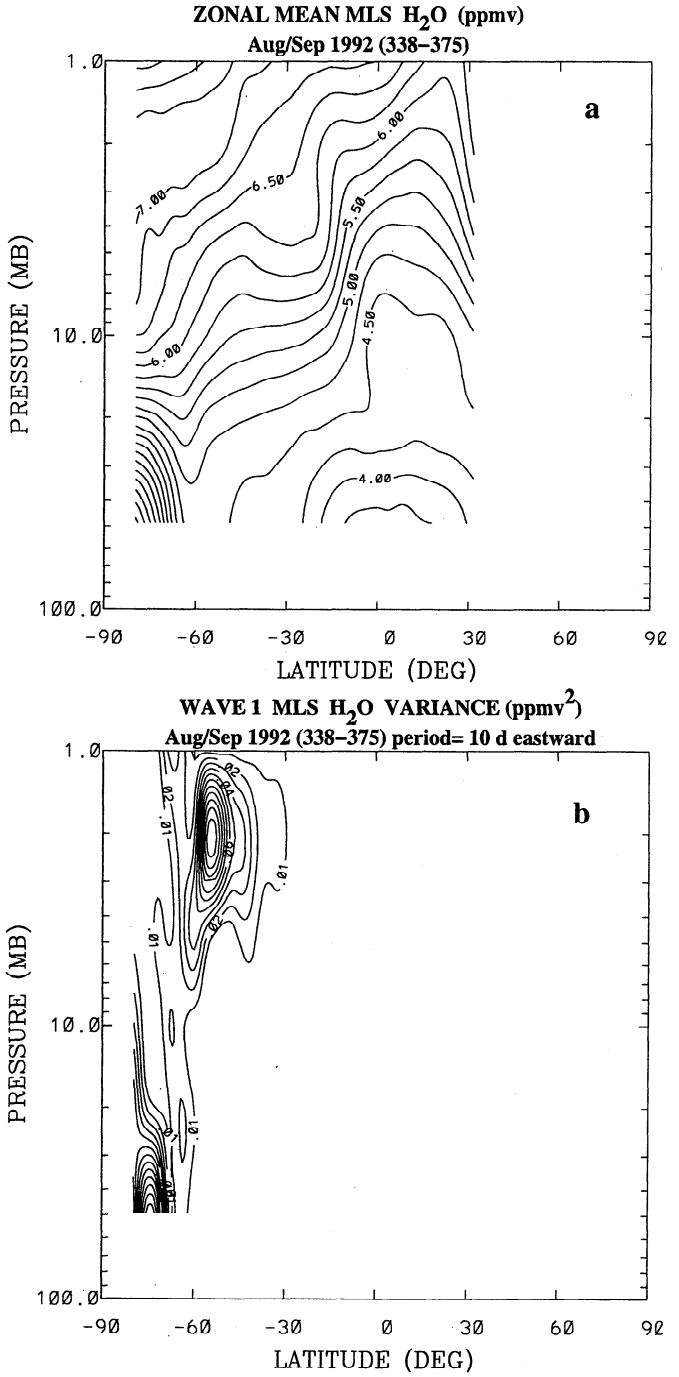

Figure 2. (a) Zonal mean water vapor (in parts per million by volume) versus pressure and latitude for August and September 1992 (UARS days 338-375). (b) As in Figure 2a but for 10-day eastward propagating water vapor variance (in parts per million by volume squared).

Kelly et al. [1991] detected differences in wintertime H_2O between the northern and southern middle-to-high latitudes from aircraft measurements. They suggest that these differences are a result of sloping convection in the presence of colder temperatures in the southern hemisphere. A similar mechanism could be at work during the summer: *Read et al.* [1995] show a small difference in winter polar MLS data at 215 hPa for the months of January and July 1992. Such differences do not appear in Plate 1 due to its coarse color resolution. It should be remembered that polar H_2O values at 215 hPa have more uncertainty than equatorial values (Read et al.).

Departures from zonal symmetry have been detected in several data sets sensitive to the upper troposphere. Studies have used outgoing longwave radiation (OLR) [e.g., *Salby and Hendon*, 1994] as an indicator of cloudy convection and generally show eastward propagating variances with a wide range of periods and largest amplitudes in wavenumbers 1-3. As discussed above, the analysis here does not have the spectral resolution to characterize the prominent spectral peaks in the 30-to 60-day range that are evident in the OLR data; however, the meridional structure of the low-wavenumber eastward variance in Plates 2a-2c is quite similar to that seen in low frequency OLR results. The isolated eastward peaks near 8 days and about 40°S latitude in Plates 2a, 2b and 2d are consistent with the enhanced OLR variance at the southern edge (30°S) of the region considered by *Slingo et al.* [1992]. Their analysis showed an enhancement in January (the period covered here) for variations with periods in the range 2-10 days. The increase in eastward variance for wavenumbers 5 and 6 is suggestive of baroclinic activity. On the basis of ECMWF analyses, *James and Anderson* [1984] found that transient eddies peak in amplitude near 250 hPa and 40°S during the December-February period and that this peak could not be explained by a dry, baroclinic theory. Moisture plays a crucial role in this region.

5.2 The Stratosphere

The 19 months of stratospheric H_2O data allow characterization of variations on timescales of a year or less. Quantitative estimates of long-period variations such as the QBO require many years of data for an accurate assessment of their effects. However, by examining H_2O together with O_3 and theoretical estimates of the circulation, it is possible to draw some conclusions about the QBO and other long-period changes.

Froidevaux et al. [1994] suggested that there is evidence of the QBO in MLS observations of 46-hPa O_3. Part of this evidence rests with a splitting of the equatorial field in the summer and fall of 1992, so that subtropical values are lower than those on the equator. This is consistent with a secondary circulation cell that exhibits downward motion at the equator and upward motion in the subtropics. There is also evidence of this, albeit much weaker, in the 46-hPa H_2O field (Plate 3h) in October 1992. Froidevaux et al. pointed out that the entire O_3 record is consistent with the modulation of equatorial upwelling with a QBO-like periodicity. However, the trend in H_2O at 46 hPa (Plates 3g and 3h) is opposite to that of O_3. To investigate this, it is useful to examine the vertical variation of the two species.

Plates 4a-4d compare zonally averaged H_2O and O_3 versus time at the equator. Part of the variation in

H_2O over 19 months is due to the upward advection of annual variations in concentration at the tropopause as described by *Mote et al.* [1996]. The vertical displacement of H_2O isopleths is often much greater than that of O_3. Below 22 hPa, this difference is most evident in December 1992. At these lower altitudes where time constants for chemical production are long, the displacement of isopleths depends on the relative angle between the wind velocity vector and the gradient in mixing ratio. Since the H_2O gradient has more of a meridional component than O_3 (as it does for the case shown in Figure 1), it is more sensitive to meridional motions than is O_3. A quantitative understanding of the role of meridional transport requires the use of a suitable transport model, which is beyond the scope of this paper.

Higher in the stratosphere, interannual effects modulate the SAO. Some measure of this can be obtained by comparing MLS results with the LIMS observations of 1978-1979. The zonal mean concentration at the equator, shown in Plate 4, is similar to that of LIMS, shown in Figure 9-24 of the World Meteorological Organization report [1986]. LIMS results, like the model results in Plate 4, show smaller variations at 2 hPa than does MLS. This, coupled with evidence (Plate 3) that the amplitude of the SAO decreased significantly after the first year of MLS observations, suggests that 1991-1992 may have been an anomalous year. Further evidence for this conclusion comes from the analysis of *Eluszkiewicz et al.* [1996] who found that the SAO in O_3 at 2 hPa decreased substantially during the September 1992 through March 1993 time period, although a stronger SAO appears later in the MLS O_3 record. *Ray et al.* [1994] pointed out that the relationship between SAO temperature and O_3 amplitudes is not easy to understand. At 2 hPa, where the two should be anticorrelated due to photochemistry, the phase difference is about 1 month instead of 3, suggesting that transport may play a role in the O_3 distribution. At 10 hPa, Ray et al. concluded that the residual mean vertical velocity is incapable of accounting for the O_3 distribution through advection of NO_X.

A somewhat different conclusion has been reached by P. Stott and A. Pardaens (personal communication, 1995) who found that they could explain the observed meridional structure of zonally averaged H_2O in the equatorial stratosphere. They used the United Kingdom Universities Global Atmospheric Modelling Programme (UGAMP) GCM that produces time-height results similar to the 2-D model results in Plate 4e, except that the phase of the SAO near 1 hPa agrees more closely with the MLS observations. The amplitude of the displacement of H_2O isopleths is quite similar in the two models and smaller than that of the observations above 5 hPa. Neither model produces a phase variation with height that matches that of the observations. This may be partly due to the coarse (about 5 km) resolution of the MLS retrievals.

H_2O in the upper stratosphere is produced through the oxidation of methane [*Le Texier et al.*, 1988]. This process is rapid enough to be observed on timescales greater than a few months. Since methane is a source of water and the chemical lifetime of methane is shorter than that of water, one might expect perturbations in H_2O to show a more rapid increase than decrease at high levels. Such does not appear to be the case. Whether the distribution of methane and the seasonal variation in its photochemical destruction can account for some of the behavior discussed above remains to be determined.

The above discussion leaves open the question of whether the large observed SAO variations in H_2O (relative to models) are caused by an enhanced residual circulation. P. Stott and A. Pardaens (personal communication, 1995) suggested that upper stratospheric interannual variations seen in the UGAMP GCM are caused by variations in gravity and Kelvin wave forcing. Clearly, forcing of the SAO is an important factor in "tuning" models so that they resemble the observations. *Randel et al.* [1994] reached a similar conclusion by comparing CCM2 simulations with UARS N_2O observations. Inclusion of other quasi-conserved species as tracers in these models will help to constrain them. Methane and nitrous oxide, both measured by UARS, are good candidates for such a procedure.

Acknowledgments. The authors thank the UARS project and our MLS colleagues for providing support. Part of this research was sponsored by NASA's Upper Atmosphere Research Satellite Project and was performed at the Jet Propulsion Laboratory, California Institute of Technology, under contract with the National Aeronautics and Space Administration.

References

Andrews, D. G., J. R. Holton, and C. B. Leovy, *Middle Atmosphere Dynamics*, pp. 313-342, Academic, San Diego, Calif., 1987.

Barath, F. T., et al., The Upper Atmosphere Research Satellite Microwave Limb Sounder Instrument, *J. Geophys. Res., 98,* 10,751-10,762, 1993.

Carr, E. S., et al., Tropical stratospheric water vapor measured by the Microwave Limb Sounder (MLS), *Geophys. Res. Lett., 22,* 691-694, 1995.

Chipperfield, M. P., and L. J. Gray, Two-dimensional model studies of the interannual variability of trace gases in the middle atmosphere, *J. Geophys. Res., 97,* 5963-5980, 1992.

Elson, L., and L. Froidevaux, The use of Fourier transforms for asynoptic mapping: Applications to the Upper Atmosphere Research Satellite Microwave Limb Sounder, *J. Geophys. Res., 98,* 23,039-23,049, 1993.

Elson, L., G. L. Manney, L. Froidevaux, and J. W. Waters, Large-scale variations in ozone from the first two years of UARS MLS data, *J. Atmos. Sci., 51,* 2867-2876, 1994a.

Elson, L., W. G. Read, and J. W. Waters, Daily, seasonal and interannual variations in upper troposphere water vapor as observed by UARS microwave limb sounder, paper presented at the Chapman Conference on Water Vapor in the Climate System, AGU, Jekyll Island, Ga., October 25-28, 1994b.

Eluszkiewicz, J., et al., Residual circulation in the stratosphere and lower mesosphere as diagnosed from Microwave Limb Sounder data, *J. Atmos. Sci., 53,* 217-240, 1996.

Froidevaux, L., J. W. Waters, W. G. Read, L. S. Elson, D.A. Flower, and R. F. Jarnot, Global ozone observations from UARS MLS: An overview of zonal mean results, *J. Atmos. Sci., 51,* 2846-2866, 1994.

Gutzler, D. S., Uncertainties in climatological tropical humidity profiles- some implications for estimating the greenhouse effect, *J. Clim., 6,* 978-983, 1993.

Harwood, R. S., et al., Springtime stratospheric water vapour in the southern hemisphere as measured by MLS, *Geophys. Res. Lett., 20,* 1235-1238, 1993.

Hasebe, F., Quasi-biennial oscillations of ozone and diabatic circulation in the equatorial stratosphere, *J. Atmos. Sci., 51,* 729-745, 1994.

James, I. N., and D. L. T. Anderson, The seasonal mean flow and distribution of large-scale weather systems in the southern hemisphere: The effects of moisture transports, *Q. J. R. Meteorol. Soc., 110,* 943-966, 1984.

Jones, R. L., J. A. Pyle, J. E. Harries, A. M. Zavody, J. M. Russell III, and J. C. Gille, The water vapour budget of the stratosphere studied using LIMS and SAMS satellite data. *Q. J. R. Meteorol. Soc., 112,* 1127-1143, 1986.

Kelly, K. K., et al., Dehydration in the lower antarctic stratosphere during late winter and early spring, 1987, *J. Geophys. Res., 94,* 11,317-11,357, 1989.

Kelly, K. K., A. F. Tuck, and T. Davies, Wintertime asymmetry of upper tropospheric water between the northern and southern hemispheres, *Nature, 353,* 244-247, 1991.

Kinnersley, J. S., and R. S. Harwood, An isentropic two-dimensional model with an interactive parameterization of dynamical and chemical planetary-wave fluxes, *Q. J. R. Meteorol. Soc., 119,* 1167-1193, 1993.

Lahoz, W. A., et al., Three-dimensional evolution of water vapour distributions in the northern hemisphere as observed by MLS, *J. Atmos. Sci., 51,* 2914-2930, 1994.

Lahoz, W. A., A. O'Neill, A. Heaps, V. Pope, R. Swinbank, R. S. Harwood, L. Froidevaux, W. G. Read, J. W. Waters, and G. E. Peckham, Vortex dynamics and the evolution of water vapour in the stratosphere of the southern hemisphere, *Q. J. R. Meteorol. Soc.*, in press, 1996a.

Lahoz, W. A., et al., Validation of UARS MLS 183-GHz H_2O measurements, *J. Geophys. Res.*, in press, 1996b.

Le Texier, H., S. Solomon, and R. R. Garcia, The role of molecular hydrogen and methane oxidation in the water vapour budget of the stratosphere, *Q. J. R. Meteorol. Soc., 114,* 281-295, 1988

Lindzen, R. S., Some coolness concerning global warming, *Bull. Am. Meteorol. Soc., 71,* 288-299, 1990.

Madden, R. A., and P. R. Julian, Observations of the 40-50 day tropical oscillation- a review, *Mon. Weather Rev., 122,* 814-837, 1994.

Mote, P. W., The annual cycle of stratospheric water vapor in a general circulation model, *J. Geophys. Res., 100,* 7363-7379, 1995.

Mote, P. W., K. H. Rosenlof, J. R. Holton, R. S. Harwood, and J. W. Waters, Seasonal variation of water vapor in the tropical lower stratosphere, *Geophys. Res. Lett., 22,* 1093-1096, 1995.

Mote, P. W., K. H. Rosenlof, M. E. McIntyre, E. S. Carr, J. C. Gille, J. R. Holton, J. S. Kinnersley, H. C. Pumphrey, J. M. Russell III, and J. W. Waters, An atmospheric tape recorder: The imprint of tropical tropopause temperatures on stratospheric water vapor, *J. Geophys. Res.*, in press, 1996.

Newell, R. E., Y. Zhu, E. V. Browell, S. Ismail, W. G. Read, J. W. Waters, K. K. Kelly, and S. C. Liu, Upper tropospheric water vapor and cirrus: Comparison of DC-8 observations, preliminary UARS MLS measurements, and meteorological analyses, *J. Geophys. Res.*, in press, 1996a.

Newell, R. E., Y. Zhu, E. V. Browell, W. G. Read, and J. W. Waters, Walker circulation and tropical upper tropospheric water vapor, *J. Geophys. Res.*, in press, 1996b.

Randel, W. J., B. A. Boville, J. C. Gille, P. L. Bailey, S. T. Massie, J. B. Kumer, J. L. Mergenthaler, and A. E. Roche, Simulation of stratospheric N_2O in the NCAR CCM2: Comparison with CLAES data and global budget analyses, *J. Atmos. Sci., 51,* 2834-2845, 1994.

Ray, E., J. R. Holton, E. F. Fishbein, L. Froidevaux, and J. W. Waters, The tropical semiannual oscillation in temperature and ozone observed by the MLS, *J. Atmos. Sci., 51,* 3045-3052, 1994.

Read, W. G., J. W. Waters, D. A. Flower, L. Froidevaux, R. F. Jarnot, D. L. Hartmann, R. S. Harwood, and R. B. Rood, Upper tropospheric water vapor from UARS MLS, *Bull. Am. Meteorol. Soc., 76,* 2381-2389, 1995.

Rind, D., E.-W. Chiou, W. Chu, S. Oltmans, J. Lerner, J. Larsen, M. P. McCormick, and L. McMaster, Overview of the SAGE II water vapor observations: Method, validation, and data characteristics, *J. Geophys. Res., 98,* 4835-4856, 1993.

Salathé, E. P., and D. Chesters, Variability of moisture in the upper troposphere as inferred from TOVS satellite observations and the ECMWF model analyses in 1989, *J. Clim., 8,* 120-132, 1995.

Salathé, E. P., D. Chesters, and Y. C. Sud, Evaluation of the upper- tropospheric moisture climatology in a general circulation model using TOVS radiance observations, *J. Clim., 8,* 2404-2414, 1995.

Salby, M. L., and H. H. Hendon, Intraseasonal behavior of clouds, temperature and motion in the tropics, *J. Atmos. Sci., 51,* 2207-2224, 1994.

Salby, M. L., D. L. Hartmann, P. L. Bailey, and J. C. Gille, Evidence for equatorial Kelvin modes in Nimbus-7 LIMS, *J. Atmos. Sci., 41,* 220-235, 1984.

Salby, M. L., H. H. Hendon, K. Woodberry, and K. Tanaka, Analysis of global cloud imagery from multiple satellites, *Bull. Am. Meteorol. Soc., 72,* 467-480, 1991.

Schäfer, J., A space-time analysis of tropospheric planetary waves in the northern hemisphere, *J. Atmos. Sci., 36,* 1117-1123, 1979.

Slingo, J. M., K. R. Sperber, J. Morcrette, and G. L. Potter, Analysis of the temporal behavior of convection in the tropics of the European Centre for Medium-Range Weather Forecasts model, *J. Geophys. Res., 97,* 18,119-18,135, 1992.

Smith, R. B., D. Rye, R. Rauber, H. Ochs, and G. Kok, Measurements of deuterium and oxygen-18 in the upper troposphere and implications for the water vapor budget of the atmosphere, paper presented at the Chapman Conference on Water Vapor in the Climate System, AGU, Jekyll Island, Ga., October 25-28, 1994.

Soden, B. J., and F. P. Bretherton, Upper tropospheric relative humidity from the GOES 6.7-μm channel: Method and climatology for July 1987, *J. Geophys. Res., 98,* 16,669-16,688, 1993.

Soden, B. J., and F. P. Bretherton, Evaluation of water vapor distribution in general circulation models using satellite observations, *J. Geophys. Res., 99,* 1187-1210, 1994.

Susskind, J., Water vapor and temperature, in *Atlas of Satellite Observations Related to Global Change,* edited by R. J. Gurney, J. L. Foster, and C. L. Parkinson, pp. 89-128, Cambridge Univ. Press, New York, 1993.

Susskind, J., J Rosenfield, D. Reuter, and M. T. Chahine, Remote sensing of weather and climate parameters from

HIRS2/MSU on TIROS-N, *J. Geophys. Res., 89,* 4677-4697, 1984.

Udelhofen, P. M., and D. L. Hartmann, Influence of tropical cloud systems on the relative humidity in the upper troposphere, *J. Geophys. Res., 100,* 7423-7440, 1995.

Wade, C. G., An evaluation of problems affecting the measurement of low relative humidity on the United States radiosonde, *J. Atmos. Oceanic Technol., 11,* 687-700, 1994.

Waliser, D. E., and C. Gautier, A satellite-derived climatology of the ITCZ, *J. Clim., 6,* 2162-2174, 1993.

World Meteorological Organization, Atmospheric ozone 1985: Assessment of our understanding of the processes controlling its present distribution and change, Rep. 16, Washington, D. C., 1986.

Zangvil, A., and M. Yanai, Upper tropospheric waves in the tropics. Part I: Dynamical analysis in the wavenumber-frequency domain. *J. Atmos. Sci., 37,* 283-298, 1980.

L.S. Elson, W. G. Read, and J. Waters, M/S 183-701, Jet Propulsion Laboratory, 4800 Oak Grove Dr., Pasadena, CA 91109.

P.W. Mote and R. S. Harwood, Department of Meteorology, The University of Edinburgh, Mayfield Road, Edinburgh, EH9 3JZ, Scotland.

J.S. Kinnersley, Department of Applied Mathematics, Box 352420, University of Washington, Seattle WA 98195-2420.

(Received May 23, 1995; revised October 12, 1995; accepted November 20, 1995.)